Available online at www.sciencedirect.com

ScienceDirect

Nuclear Physics A 1018 (2022) 122359

NUCLEAR PHYSICS A

www.elsevier.com/locate/nuclphysa

Total absorption spectroscopy measurement on neutron-rich ^{74,75}Cu isotopes

F. Naqvi [a,b,*,1], S. Karampagia [a,2], A. Spyrou [a,b,c], S.N. Liddick [a,b,c,d], A.C. Dombos [a,b,c], D.L. Bleuel [e], B.A. Brown [a,b,c], L. Crespo Campo [f], A. Couture [g], B. Crider [a], T. Ginter [a], M. Guttormsen [f], A.C. Larsen [f], R. Lewis [a,d], P. Möller [g], S. Mosby [g], G. Perdikakis [h,a], C. Prokop [a,d], T. Renstrøm [f], S. Siem [f]

[a] *National Superconducting Cyclotron Laboratory, Michigan State University, East Lansing, MI 48824, USA*
[b] *Joint Institute for Nuclear Astrophysics, Michigan State University, East Lansing, MI 48824, USA*
[c] *Department of Physics and Astronomy, Michigan State University, East Lansing, MI 48824, USA*
[d] *Department of Chemistry, Michigan State University, East Lansing, MI 48824, USA*
[e] *Lawrence Livermore National Laboratory, 700 East Avenue, Livermore, CA 94550-9234, USA*
[f] *Department of Physics, University of Oslo, NO-0316 Oslo, Norway*
[g] *Los Alamos National Laboratory, Los Alamos, NM 87545, USA*
[h] *Central Michigan University, Mount Pleasant, MI 48824, USA*

Received 24 February 2021; received in revised form 31 October 2021; accepted 15 November 2021
Available online 19 November 2021

Abstract

This paper reports on the first β-decay study of ^{74,75}Cu isotopes using the technique of total absorption spectroscopy (TAS). The experiment was performed at the National Superconducting Cyclotron Laboratory at Michigan State University using the Summing NaI(Tl) (SuN) detector. The Cu isotopes are good candidates to probe the single-particle structure in the region because they have one proton outside the $Z = 28$ shell. Comparing the β-decay intensity distributions in the daughter Zn isotopes to the theoretical predictions provides a stringent test of the calculations. The nuclei in this region are also identified as play-

* Corresponding author at: National Superconducting Cyclotron Laboratory, Michigan State University, East Lansing, MI 48824, USA.
E-mail address: fnaqvi@mit.edu (F. Naqvi).
[1] Present address: Department of Nuclear Science & Engineering, Massachusetts Institute of Technology, Cambridge, Massachusetts 02139, USA.
[2] Present address: Department of Physics, Grand Valley State University, Allendale, Michigan 49401, USA.

https://doi.org/10.1016/j.nuclphysa.2021.122359

ing an important role in the astrophysical r-process. The measured β-decay intensity distributions provide essential nuclear physics inputs required to better understand heavy element nucleosynthesis.

Keywords: Beta decay; Total absorption spectroscopy; Beta-decay intensity

1. Introduction

The isotopes between $N = 40$ and $N = 50$ shell closures present a rich landscape for understanding different aspects of nuclear structure. This region is marked by sudden structural changes which are mainly attributed to the role of the residual proton-neutron interaction. Just two neutrons above the apparent $N = 40$ gap in $Z = 28$ nuclei [1], ^{70}Ni shows a sudden onset of collectivity [2,3]. Similar behavior is also observed in the Ge and Se chains [4–7]. This was explained as the consequence of a strong monopole interaction between the $\pi f_{5/2}$-$\nu g_{9/2}$ and $\pi f_{7/2}$-$\nu g_{9/2}$ single-particle orbitals [2,8–11]. An extensive migration of single-particle energy states is prevalent in the whole region having implications on the question of robustness of the $Z = 28$ shell gap while approaching ^{78}Ni [12]. Therefore, a large effort has been devoted over the last decade to map this evolution. Information on the excited states in odd-mass Zn isotopes populated in the β decay of Cu nuclei having one proton in $Z = 28$ shell, is known up to $A = 77$ [13–16]. The experimental data proves that the ground state spin and parity for the odd-mass Cu nuclei remains $3/2^-$ until $A = 73$ and then an inversion to $5/2^-$ takes place at $N = 46$ as a result of the crossing of $\pi f_{5/2}$ and $p_{3/2}$ orbitals [17,18]. This transitional point calls for an exhaustive investigation of the decay of ^{75}Cu and isotopes around.

So far, the β-decay properties of ^{74,75}Cu were studied using high-resolution γ-spectroscopy methods [19,20,15]. The measurements done with high-resolution detectors often suffer from the so-called *Pandemonium effect* [21]. Due to the limitations in the efficiency of these detectors, low-intensity and/or high-energy γ rays are difficult to detect. As a consequence, the extracted β-decay intensities are artificially enhanced for low excitation energies. The total absorption spectroscopy (TAS) technique is widely accepted as a solution to minimize the *Pandemonium effect* by measuring the sum of γ-ray energies in a decay cascade rather than only the individual γ rays [22,23]. In this paper, we report on the first total absorption spectroscopy measurements on neutron-rich ^{74,75}Cu. The extracted β-intensity distributions, I_β are also converted to the corresponding Gamow-Teller transition strength distributions, B(GT).

Looking from an astrophysical point of view, the neutron-rich Cu isotopes play an important role in the rapid neutron capture process (r-process) which is known to be responsible for creating more than half of the heavy elements [24,25]. The r-process is believed to progress through neutron captures and competing β decays. During the r-process flow, matter is known to accumulate around neutron-magic-numbers, and as a result form peaks in the final abundance distribution. Sensitivity studies have shown that nuclei around shell-closures have a larger impact on the abundance pattern [26]. The nuclei included in the present work are close to the $N = 50$ shell which results in the first r-process peak. These nuclei may have multiple nucleosynthetic origins [27] and it is therefore important to have a good handle of the nuclear physics input in the region if we can hope to disentangle the contributions from different astrophysical processes. Despite the widely proclaimed importance and the need for nuclear-data input to study the r-process, the majority of the important neutron-rich r-process isotopes are not accessible

experimentally. Therefore, robust nuclear models are required to predict the nuclear properties in the region where no experimental data is present. To ensure the reliability of the models, a systematic testing in the region of measured experimental data is of paramount importance. The main nuclear quantities which are essential for the r-process models include masses, neutron-capture rates, β-decay half-lives, and β-delayed neutron emission probabilities [26,28]. For any given isotope, the latter two quantities are obtained by integrating the β-decay strength function over different limits of excitation energy in the daughter nucleus. The β-decay strength function also finds its application in calculating the reactor decay heat and the structure studies of the nuclei decaying via β emission [29].

In recent β-decay measurements, a strong γ emission from the states 2 - 3 MeV above the neutron-separation energy in daughter nuclei has been observed [30–34]. In some cases, this competition between the γ decay and neutron emission from the neutron-unbound states is mainly attributed to the difference in wavefunctions of the daughter states and the states in its nearby isotope with one less neutron [33,34]. Structure effects are therefore critical in understanding the beta-delayed neutron emission process. In Ref. [33], the observed γ emission from states above the neutron separation energy in the decay of ^{70}Co suggests that these states decay via a competition between γ emission and neutron emission. Therefore, the assumption typically made in theoretical calculations that neutron-unbound states predominantly decay via neutron emission may not always be valid. These considerations will affect the theoretically predicted P_n value. For this reason, the experimental determination of the γ-emission spectrum using the TAS method in neutron-rich nuclei becomes all the way more important. Our measurement of the I_β in ^{74,75}Cu isotopes gives a means to test the theoretical models in the region of rapid structural changes. The experimental results in this paper are compared to shell-model calculations using two different interactions, JUN45 [35] and *jj*44b [36]. In addition, the experimentally extracted I_β and B(GT) are compared to the quasiparticle random phase approximation (QRPA) predictions [37]. The QRPA model provides a global description of the β-decay properties all over the nuclear chart. In the case of the neighboring ^{70}Co nucleus decaying into ^{70}Ni [33], its limitation in reproducing the experimental I_β values at high excitation energies emphasizes the need of testing it for surrounding nuclei, including ^{74,75}Cu.

In the following section, a description of the experimental setup and technique is given. Details on the analysis methods and experimental results are presented in Sec. 3. Section 4 provides discussion on the comparison of experimentally extracted I_β and B(GT) with theoretical predictions using the JUN45 and *jj*44b shell-model interactions and the QRPA approach. Finally, conclusions are given in Sec. 4.

2. Experimental method

The ^{74,75}Cu nuclei were produced in an experiment performed at the Coupled Cyclotron Facility of the National Superconducting Cyclotron Laboratory (NSCL), USA. Fragmentation of a primary beam of ^{86}Kr at an energy 140 MeV/u on a ^{9}Be target of 376 mg/cm^2 thickness yielded the neutron-rich Cu isotopes along with other reaction products. Ions were separated by the A1900 fragment separator [38] and delivered to the SuN detector setup for β decays.

To identify isotopes in the secondary beam, time-of-flight and energy loss techniques were used. Time-of-flight between a scintillator detector kept at the dispersive focal plane of the A1900 fragment separator and two silicon PIN detectors upstream of SuN determined the velocity and thus the A/Q ratio of the beam particles. For a complete identification, the Z of the fragments was provided by the energy loss measurement in the same two Si PIN detectors. The identifi-

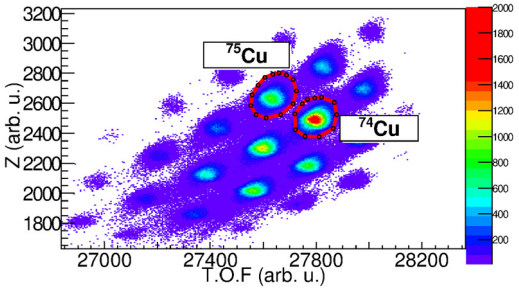

Fig. 1. Particle identification plot for the fragments produced in the experiment. ^{74,75}Cu isotopes are marked in red. (For interpretation of the colors in the figure(s), the reader is referred to the web version of this article.)

cation plot for the Cu isotopes along with its neighboring nuclei produced in the experiment is shown in Fig. 1. For β-decay measurements, the relativistic ions were first slowed down in a $\sim$ 2.5 mm thick Al degrader placed at the front of the Si PIN detectors and then implanted in a 1 mm thick double-sided silicon detector (DSSD) surrounded by SuN [39]. Another Si surface barrier detector used as the veto detector, of 2 cm diameter and 0.5 mm thickness, was placed 1.9 cm downstream of the DSSD to reject the light particles coming along with the beam. The thickness of the Al degrader was chosen to ensure that the implantation of most of the ions was in the middle of the DSSD.

The DSSD is segmented into 16 strips on the front and 16 strips on the back side to enable position determination. The width of each strip is 1.22 mm and the DSSD type is Micron-BB8(DS). Dual-gain preamplifiers enabled the detection of high-energy implantations ($\sim$10 GeV) and low-energy β decays ($<$5 MeV). The energy threshold for detecting electrons in DSSD was 200 keV. The coincidence window of SuN and DSSD was kept 2 μs to reduce the room background. To correlate an ion implantation to its β decay, the beam spot was defocused in order to cover the whole area of the DSSD which minimizes the probability of multiple implantations in the same pixel. For this purpose, the total rate on the DSSD was also kept less than 100 pps at all times during the experiment. The implantation rate for ^{74}Cu and ^{75}Cu was around 10 to 12 pps.

γ decays of the excited states following the β decay were registered in SuN detector. SuN is a summing detector made of 8 optically isolated NaI(Tl) crystals. It is cylindrical in shape with 16 in. in diameter and 16 in. in length and has a 1.8 in. wide central bore hole along the beam axis. SuN is divided into two halves having 4 segments each and the individual segments are read by 3 photomultiplier tubes (PMTs). Such a compact geometry of the whole detector makes it an ideal tool to do γ-summing experiments. A plot with SuN's full-energy peak efficiency for single and multiple γ rays in the present setup are shown in Fig. 2. Different curves represent the dependence of summing efficiency on the multiplicity of the γ rays. Ref. [39] provides a detailed description of SuN and the results from its commissioning experiment. It should be noted that the setup used in [39] was different from the one used in the present work. The present setup includes additional material in the SuN borehole (e.e. DSSD, veto detector, mounts) that reduce the overall efficiency of SuN. Results focused on the decay of ^{70}Co produced in the same experiment were already presented in Refs. [33,40].

3. Analysis and results

All 24 PMTs of SuN were gain matched prior to the start of the experiment and then the segments were energy calibrated using standard ^{60}Co, ^{137}Cs, and ^{228}Th sources. For gain matching

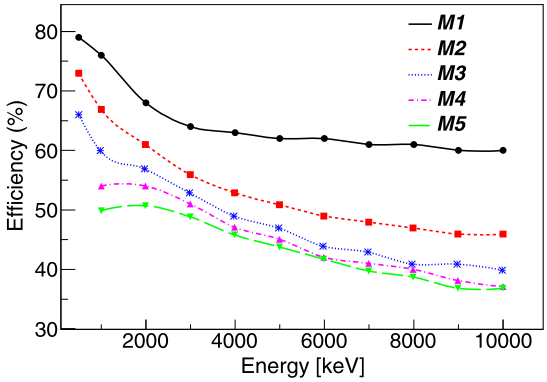

Fig. 2. SuN's full-energy peak efficiency for detecting single and multiple γ rays in present setup. Different curves represent the dependence of summing efficiency on the multiplicity of the γ-ray cascade.

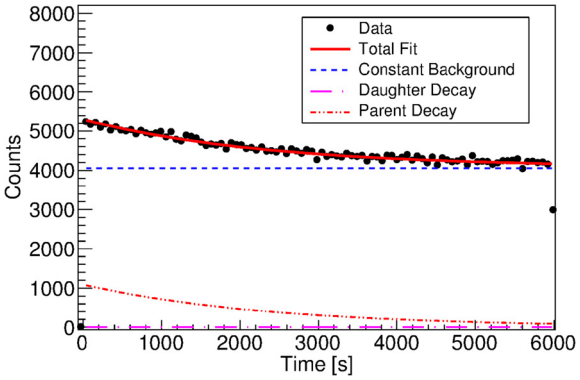

Fig. 3. Lifetime curve for the β-decay of ^{74}Cu. Data was fit with a constant background and a two-component function for exponential decay of parent nucleus and growth and decay of daughter ^{74}Zn isotope.

the 16 strips on each side of the high-gain preamplifier of the DSSD (for β decays), α sources of ^{228}Th and ^{241}Am were used. The first step after calibrating all the detectors is to properly correlate an implantation event with its β-decay electron. In the present analysis, three main conditions were implemented to obtain these "real" correlations. First, a spatial condition of a β-decay event happening in the same pixel as that of an implantation is required for a correlation. Second, if a pixel registers two implantations within 1 second of each other, that event is marked as a back-to-back implantation and is rejected. Finally, a β-decay event is considered valid only if it happens within 6 seconds after the implantation. The time limit of 6 seconds was chosen to maximize the counts of the Cu parents at the expense of increased random correlations due to everything else being implanted. This condition also reduces the contributions from the daughter and grand-daughter activities due to the longer half-lives of 95.6(12) s and 10.2(2) s for the ^{74,75}Zn isotopes, respectively [41,42]. To estimate the randomly correlated background counts, the same spectra were created by running the analysis backward in time.

The decay curves of ^{74}Cu and ^{75}Cu shown in Fig. 3 and Fig. 4 were fit using a linear background obtained from random correlations and a two-component curve consisting of an exponential decay for parent activity and the growth and decay of the daughter contributions. The re-

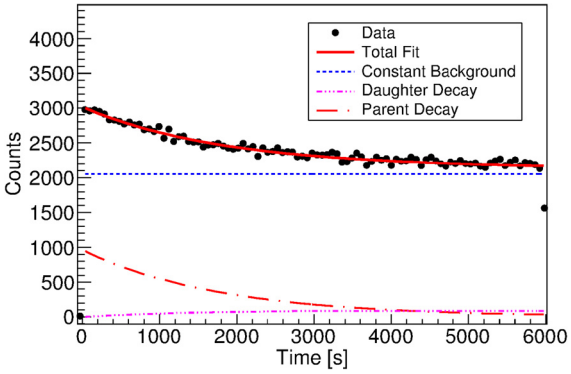

Fig. 4. Lifetime curve for the β-decay of ^{75}Cu. Data was fit with a constant background and a two-component function for exponential decay of parent nucleus and growth and decay of daughter ^{75}Zn isotope.

sulting $T_{1/2}$ = 1.62(5) s for the ^{74}Cu decay and $T_{1/2}$ = 1.23(4) s for the ^{75}Cu decay compare well with previous literature values of 1.63(5) s and 1.224(3) s, respectively from [43–46,20,47,15].

To obtain the β-decay intensities as a function of the excitation energy in the daughter nucleus, three spectra were used; the total absorption spectroscopy spectrum, the spectrum of all individual SuN segments, and the hit-pattern of the segments. The TAS spectrum is obtained by adding the total energy deposited in SuN on an event-by-event basis. Since the energies of all the γ rays originating from a single cascade are added together to give rise to the TAS spectrum, it is sensitive to the levels populated in the decay. A sum-of-segments spectrum is constructed by adding the histograms for all the segments, and therefore it is sensitive to the individual γ rays in a cascade. The hit-pattern spectrum denotes the number of segments registering energy during an event. The centroid of the hit-pattern spectrum relates to the γ multiplicity of a cascade. The higher (lower) the centroid, the higher (lower) the γ multiplicity of the event. A study of the relationship between γ multiplicity and the hit pattern of SuN can be found in Ref. [39]. The TAS, sum-of-segments, and hit-pattern spectra corresponding only to the decay of ^{74,75}Cu were obtained by subtracting the random correlations from the raw spectrum.

The GEANT4 package [48] was used to simulate the response function of current experimental setup. Both γ and electron penetration was considered for SuN's response while for DSSD only electrons were simulated. The code with full detector geometry was tested by comparing with the experimental α spectra in the DSSD and γ spectra in SuN for ^{228}Th and ^{60}Co sources, respectively, and a good agreement was obtained. After establishing the SuN detector response function, each decay cascade from the known level scheme for the decay of ^{74,75}Cu [41,42] was simulated. At first, a comparison between the experimental data and the simulation was made with the decay cascades and I_β known in literature. For the decay of ^{75}Cu, the NNDC simulation spectrum is drawn along with the experimental TAS spectrum in Fig. 5. The Q_β value of this decay is 8.09 MeV and the neutron separation energy, S_n, for ^{75}Zn is 4.87 MeV [42]. In previous studies, two excited states above the S_n of ^{75}Zn were observed to be populated in the β decay of ^{75}Cu [15]. Therefore, the inclusion of excited levels up to 5.022 MeV [42] in the simulation gave a good agreement with the experimental data. The high-energy tail observed above 5 MeV is due to the detection of high-energy β-decay electrons in SuN.

For the decay of ^{74}Cu, a large discrepancy was observed between the experimental data and the simulated spectra obtained from only the NNDC level scheme and I_β (see Fig. 6). Such a mismatch points to the incomplete decay scheme. Though this decay has a large Q_β value of 9.7

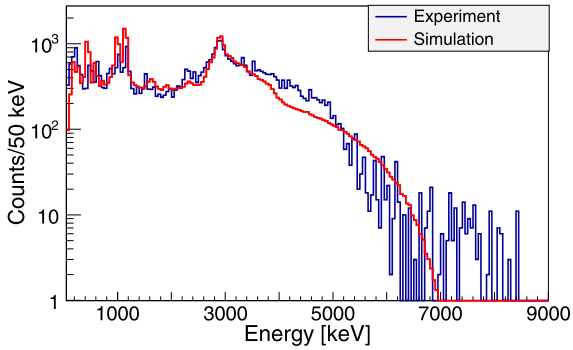

Fig. 5. Comparison of the experimentally obtained TAS spectrum for ^{75}Cu with the known level scheme and β-decay intensities from NNDC [42].

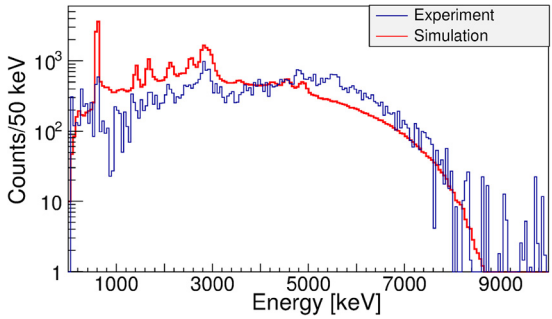

Fig. 6. Comparison of the experimentally obtained TAS spectrum for ^{74}Cu with the known level scheme and β-decay intensities from NNDC [41]. The observed discrepancy is due to the incomplete level scheme and the *Pandemonium effect*.

MeV, the highest-energy level known to be populated in ^{74}Zn is only at 5.63 MeV [41]. As the S_n for the daughter ^{74}Zn is 8.3 MeV, a large number of high-energy levels which are expected to be populated are missing from the decay scheme due to the *Pandemonium effect*. The conclusion which can be drawn from such a comparison is that there is a need for adding levels above 5.63 MeV in the β decay of ^{74}Cu to get a complete description of the β-feeding intensities. Whereas in ^{75}Cu, levels populated in the β decay appear to be accurately known.

To extract the I_β of ^{75}Cu, the experimental TAS, sum-of-segments and hit-pattern spectra corresponding to the different cascades were simultaneously fit to the experimental data to minimize a global χ^2, which is defined as:

$$\chi^2_{global} = \sum_i \sum_j \left(\frac{e_{ij} - \sum_k p_k s_{jk}}{\sqrt{e_{ij}}} \right)^2 \tag{1}$$

Here, the index i is for the three spectra included in the fit. e_{ij} and s_{jk} are the number of counts in bin j of experimental and k^{th} cascade of the simulated spectra, respectively. The quantity p_k is the probability of cascade k and is varied until a minimization is achieved. The starting values for p_k are taken from NNDC. After the fitting routine is complete, the resulting p_k denotes the product of the β-feeding intensity, I_β, of the level depopulated by cascade k and the branching ratio, B_k, of that cascade, i.e., $p_k = I_\beta B_k$. Since the sum of branching ratios of all the cascades

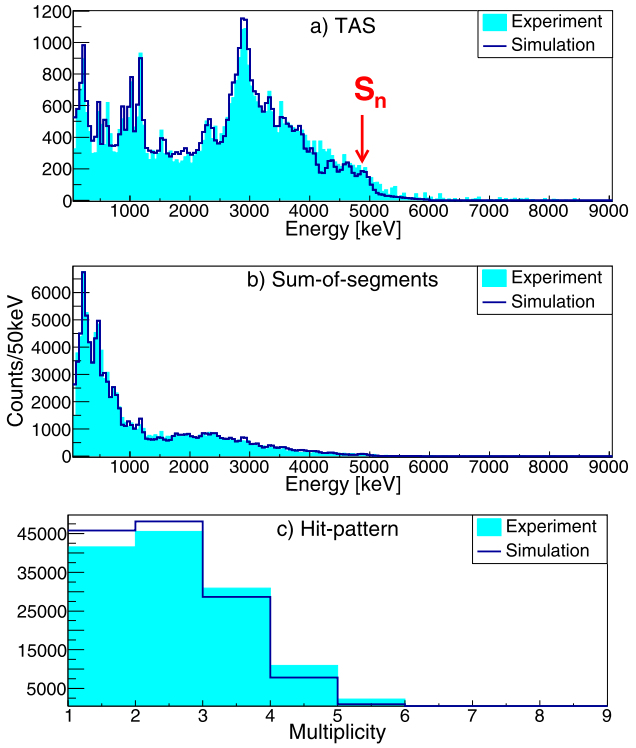

Fig. 7. TAS spectrum (a), sum-of-segments spectrum (b), and the hit-pattern (c) obtained in the decay of ^{75}Cu following subtraction of random correlations. Shaded spectra are the experimental data and the fit after χ^2 minimization of the simulated decay pattern is shown in the blue solid line. The S_n value for ^{75}Zn is 4.87 MeV. The high-energy tail observed above 5 MeV is due to the electron energies getting summed up in SuN.

originating from a single state is unity, the sum of all p_k for a given level gives the I_β of that state. For more details about the minimization procedure, refer to Ref. [49]. Results obtained after the χ^2 minimization for the decay of ^{75}Cu are presented in Fig. 7.

A recent detailed high-resolution spectroscopy study of ^{74}Cu β decay [19] extends the level scheme of daughter ^{75}Cu to 5.72 MeV and adds a total of 29 new levels to the level scheme given in NNDC [41]. The results reported in Ref. [19] were incorporated in the present simulation. To account for the missing decays in ^{74}Zn, 25 pseudo levels were first added in the decay scheme with energies ranging from 5.8 MeV to 8.2 MeV, every 100 keV and then the χ^2 minimization was done. Above 5.8 MeV, a quasicontinuum was assumed to exist and each added level above that energy is a representative of all the levels lying in 100 keV energy interval. To simulate the γ decays from these 25 pseudo levels, a Monte-Carlo method based code called DICEBOX [50] was used. It is a statistical model code which produces random deexcitation paths for each excited state. As user inputs DICEBOX takes information such as energies, spin-parities and relative γ-ray intensities to simulate the decay of known discrete levels. For simulating the decay of pseudo states added in quasicontinuum, the program uses statistical properties of nuclear level density (NLD) and γ-ray strength functions (γSFs) for $E1$, $M1$ and $E2$ transitions. The decay within quasicontinuum and the decay of the levels in quasicontinuum to a known discrete level are defined by the γ-ray strength function and the transitions between known levels are deter-

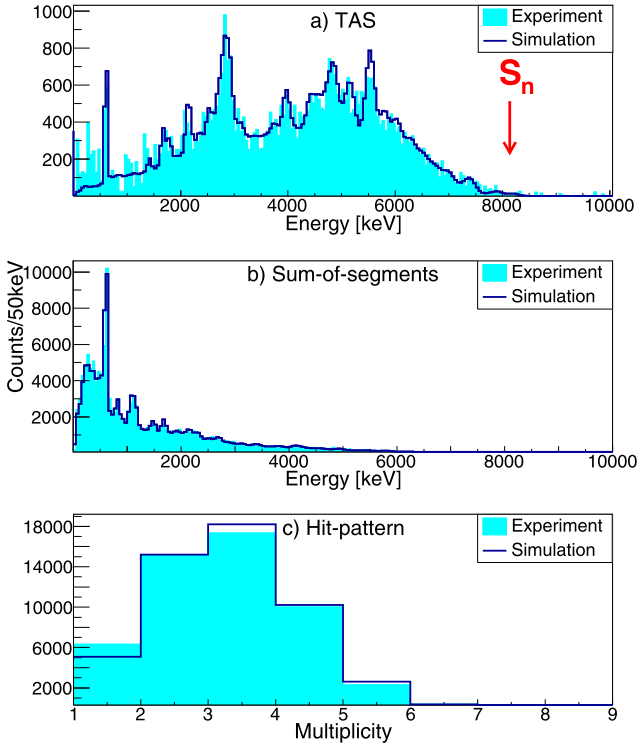

Fig. 8. TAS spectrum (a), sum-of-segments spectrum (b), and the hit-pattern (c) obtained in the decay of ^{74}Cu. Shaded spectra are the experimental data and the fit after χ^2 minimization of the simulated decay pattern is shown in the blue solid line. The neutron-separation energy, S_n for the daughter ^{74}Zn nucleus is 8.3 MeV, hence no levels are populated above that value in TAS spectrum.

mined by the relative γ-ray intensities. Decay paths for each excited state populated in the decay of ^{74}Cu obtained using this procedure were then fed to GEANT4 to give TAS, sum-of-segments and multiplicity spectra. The improvement in the fit after adding pseudo levels to the NNDC level scheme of ^{74}Zn is shown in Fig. 8 and the extracted β-feeding intensities are presented in Fig. 10(a). It should be noted that the first excited state in ^{74}Zn is at 606 keV but the TAS spectrum (see Fig. 8(a)) contains a few counts in the low-energy region below 400 keV. By gating on this region and looking at the experimental lifetime data, it was concluded that the half-life of 606 keV level and the counts below 400 keV is not the same. This observation indicates that the latter do not belong to the β decay or β-delayed neutron-emission of ^{74}Cu. For comparison, raw spectrum, random correlation spectrum and real correlation spectrum obtained after subtracting the former two for the decay of ^{74}Cu are presented in Fig. 9. As the random correlation spectrum and the raw spectrum have comparable number of counts in the low-energy region, the obtained real correlation spectrum has an uncertainty of $50-90\%$ in the E$<$ 400 keV range. Due to low statistics and high uncertainty, no further analysis could be done and no affirmation could be made on the origin of the low-energy background and, therefore, the region below 400 keV in TAS spectrum was excluded from the χ^2 fit. Prior to this work, β-delayed neutrons from ^{74}Cu were observed in Ref. [46] but no β-delayed neutron-emission probability, P_n, was extracted. However, in Ref. [51], this value is reported to be 0.075(16)%. In addition, the available theoret-

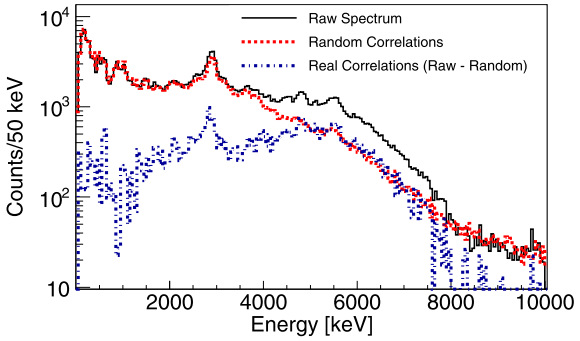

Fig. 9. Raw spectrum (solid line), random correlation spectrum (dashed line) and real correlation spectrum (dashed-dotted line) obtained after subtracting the former two for the decay of ^{74}Cu.

ical prediction by Borzov et al. estimates this value to be small but greater than zero [52]. Due to a very small P_n value for the decay of ^{74}Cu, no β-delayed neutron-emission components were fitted to the experimental spectra.

The ground state to ground state (gs-gs) transitions in both ^{74,75}Cu decay are tentatively assigned as first forbidden decays. Considering the decay of ^{74}Cu to ^{74}Zn, the transition is from $(2, 3)$ to 0^+ and for ^{75}Cu the gs-gs decay is a $(5/2^-)$ to $7/2^+$ transition. Since, both transitions are forbidden, their contribution to respective I_β is expected to be small. Though the β particles deposit energy in SuN, due to the continuous character of the energy deposition, SuN is not sensitive to small values of gs-gs transition. Hence, a reliable estimate of the gs-gs contribution is not possible in both the nuclei in present setup and therefore the corresponding feedings were not included in our fits.

The quoted errors in the experimental I_β values for both nuclei shown in Fig. 10 are a convolution of $\sim$10% uncertainty in the summing efficiency of SuN and the statistical uncertainty in the number of counts in experimental TAS spectrum. For ^{74}Cu, the statistical uncertainty ranges from 4% to 15% for γ-ray energies up to 8 MeV, whereas for ^{75}Cu, it varies between 3% to 13% for the entire range of 5.02 MeV. There is no clear indication of the population of excited levels in ^{74}Zn through the β-delayed neutron emission branch of ^{75}Cu. Therefore, for ^{75}Cu decay an extra 3.5 % uncertainty was added to the final results to account for the β-delayed neutron emission probability suggested in Reeder et al. [47].

4. Discussion

The experimental I_β values are converted to the corresponding B(GT) following the procedure described in Ref. [23]. The comparison of experimental I_β and the B(GT) with QRPA and shell-model approaches are shown in Fig. 10 and Fig. 11, respectively. The QRPA calculation is done using the folded-Yukawa QRPA model [37] and assumes identical shapes of the parent and daughter nuclei. A quenching factor of 0.55 was used for these calculations. Only the contributions from the allowed Gamow-Teller transitions are accounted for. Looking at the cumulative I_β intensity plots, experimental data indicates a strong population of the states around 3 MeV in ^{74}Zn and at 1 MeV in ^{75}Zn. This observation is supported by the QRPA prediction as well, however I_β of states below 3 MeV in the decay of ^{74}Cu and below 1 MeV in the decay of ^{75}Cu are not reproduced by the theory. An overall good agreement was obtained between the experimental B(GT) values and QRPA calculations as presented in Fig. 11.

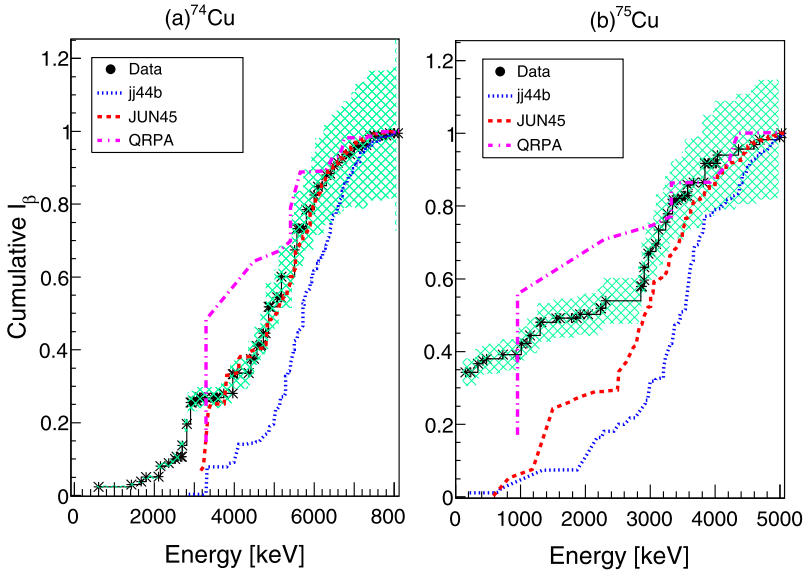

Fig. 10. The experimentally extracted cumulative β-decay intensity as a function of excitation energy in ^{74}Zn following subtraction of random correlations (a) and ^{75}Zn (b) populated in the β decay of ^{74}Cu and ^{75}Cu, respectively. The theoretical calculations done using JUN45 (red, dashed line) and *jj*44b (blue, dotted line) shell-model interactions and QRPA approach (magenta, dash-dotted) are plotted with the experimental data (black crosses). The shaded region corresponds to the uncertainty in the experimental values.

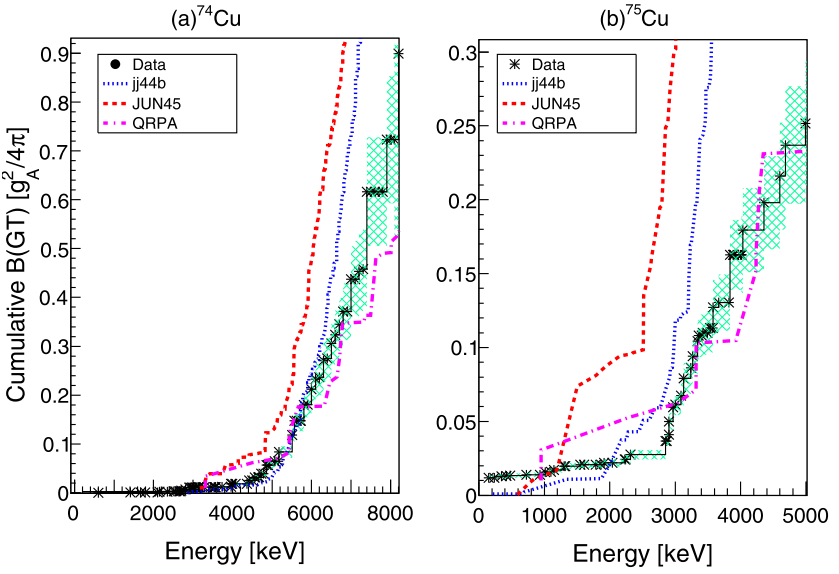

Fig. 11. The cumulative B(GT) as a function of excitation energy in ^{74}Zn (a) and ^{75}Zn (b) daughter nuclei. The theoretical calculations done using JUN45 (red, dashed line) and *jj*44b (blue, dotted line) shell-model interactions and QRPA approach (magenta, dash-dotted line) are plotted for comparison with the experimental data (black crosses). The shaded region corresponds to the uncertainty in the experimental values.

The ground state and the β-decay properties of ^{74,75}Cu, as well as the level scheme of their daughter nuclei were calculated using the NuShellX@MSU code [53]. Two different effective interaction Hamiltonians were used, *jj*44b [36] and JUN45 [35]. These Hamiltonians have been developed for the *jj*44 model space which is based upon a ^{56}Ni core with the valence protons and neutrons occupying the $1f_{5/2}$, $2p_{1/2}$, $2p_{3/2}$ and $1g_{9/2}$ single particle orbitals. Both Hamiltonians predict the ground state spin and parity of ^{75}Cu to be $5/2^-$, in agreement with experiment [18]. The experimental ground-state spin and parity of ^{74}Cu is (2, 3) [20]. The *jj*44b Hamiltonian predicts a 3^- ground state and the first two excited states, 6^- and 2^- at 0.136 MeV and 0.169 MeV, respectively. The JUN45 Hamiltonian predicts a 5^- ground state and the first two excited states, 3^- and 2^- very close in energy to the ground state at 0.008 MeV and 0.044 MeV, respectively. The experimental (2,3) is not inconsistent with these results given their close spacing. The calculated β-decay half-life of ^{74}Cu is 1.56 s for *jj*44b and 0.73 s for JUN45, while the experimentally obtained half-life in this work is 1.62(5) s. The half-life of ^{75}Cu using the *jj*44b interaction is predicted at 0.52 s and using the JUN45 interaction at 0.3 s, while the experimental one is 1.23(4) s.

For the β-decay calculations the standard quenching factor, 0.6 was used, based on the previous calculations in sd and pf shells [54,55]. The cumulative β-decay feeding intensity of ^{74,75}Cu in their daughter nuclei, as a function of excitation energy, shows that both interactions give a lower intensity, than the one observed, for low-lying states. This might be because some of these states are fed by first-forbidden decays which can not be calculated in the present approach. For example, for ^{74}Zn and for the *jj*44b interaction, the first allowed β-decay transition to a state in ^{74}Zn is at 2.880 MeV, with 7 states below that energy, which can be populated by first-forbidden transitions. For the JUN45 interaction, the first allowed decay is at 3.171 MeV, with 10 states below that, which can be reached only through first-forbidden transitions. For ^{75}Zn, for the *jj*44b interaction, the energy of the first state with an allowed β-decay transition is at 0.215 MeV and there is 1 state, below that, which the ground state of ^{75}Cu can populate by first-forbidden transitions. For the same nucleus and the JUN45 interaction, the first state with allowed β-decay transition is at 0.585 MeV, with only 2 states below, where we can have first-forbidden transitions.

The calculated cumulative B(GT) is much larger than experiment for high excitation energies. Between the two shell-model interactions the *jj*44b agrees better with the low excitation experimental data. In the decay of ^{74}Cu, for both JUN45 and *jj*44b interactions, the first Gamow-Teller strength, around 3 MeV, comes mostly from $\nu 2p_{1/2}$ to $\pi 2p_{3/2}$, but also from $\nu 2p_{3/2}$ to $\pi 2p_{3/2}$ transitions. The Gamow-Teller strength around 5 MeV is mainly due to $\nu 2p_{1/2}$ to $\pi 2p_{3/2}$ transitions and a smaller contribution from $\nu 1f_{5/2}$ to $\pi 1f_{5/2}$ transitions. The steep increase of the calculated cumulative B(GT) values above 5 MeV, which leads to an overestimation of the experimental data, is dominated by $\nu 2p_{1/2}$ to $\pi 2p_{3/2}$ transitions.

For the ^{75}Cu nucleus, the *jj*44b interaction, gives a Gamow-Teller strength around 1.3 MeV, which comes mainly from $\nu 2p_{1/2}$ to $\pi 2p_{3/2}$ transitions, with considerable contributions from $\nu 2p_{3/2}$ to $\pi 2p_{3/2}$ and $\nu 2p_{3/2}$ to $\pi 2p_{1/2}$ orbitals. The Gamow-Teller strengths for the excited states between 3−4 MeV, are mainly attributed to $\nu 2p_{1/2}$ to $\pi 2p_{3/2}$ transitions, while the $\nu 2p_{3/2}$ to $\pi 2p_{3/2}$ transitions are responsible for the Gamow-Teller strengths around 4−5 MeV. The JUN45 Hamiltonian gives a very strong Gamow-Teller strength around 1.5 MeV, which comes mainly from the $\nu 2p_{1/2}$ to $\pi 2p_{3/2}$ transitions, with smaller contribution from the $\nu 2p_{3/2}$ to $\pi 2p_{3/2}$ transition. The Gamow-Teller strengths for the excited states between 2.5−3.5 MeV, are mainly attributed to $\nu 2p_{1/2}$ to $\pi 2p_{3/2}$ transitions and less to $\nu 2p_{3/2}$ to $\pi 2p_{3/2}$ transitions.

5. Conclusions

In summary, the β-decay intensities and B(GT) values for ^{74,75}Cu isotopes were extracted for the first time using the total absorption spectroscopy technique. The experiment was done using the SuN detector at the National Superconducting Cyclotron Laboratory. Extracting the I_β values in neutron-rich Cu isotopes are interesting in view of their vicinity with the ^{70}Co nucleus, where considerable β-decay intensities were observed for states above the neutron-separation energy in the daughter nucleus [33]. In our investigation of the decay of ^{74,75}Cu, however, no such observation was made in line with the interpretation of [33]. Experimental data clearly points toward the insufficiency of the known level schemes and I_β values for both nuclei. For a theoretical comparison, the QRPA model, which is commonly used in astrophysical calculations, is shown to well reproduce the experimental I_β and B(GT) values for the decay of both $A = 74$ and 75 Cu isotopes. However, the *jj*44b and JUN45 shell-model Hamiltonians overestimate the experimental cumulative B(GT) values for high excitation energies, while the JUN45 Hamiltonian overestimates the experimental results, already from lower excitation energies. In a previous study [49], where the β decay of ^{76}Ga was studied using the same Hamiltonians, a quenching factor of 0.4 was applied to both Hamiltonians, based on the comparison of the experimental β-decay half-lives and the calculated ones. In our case, the consideration of this quenching factor improves the agreement with the data, however the discrepancy remains significant. The insufficiency of shell-model calculations to reproduce the experimental data could be due to the truncation of the model space. The calculated B(GT) values give strong contributions in the excited region, mainly due to $\nu 2p_{1/2}$ to $\pi 2p_{3/2}$ transitions. Thus, a subject of future study can be whether one obtains a better comparison to experiment by raising the $p_{1/2}$ single-particle energy.

CRediT authorship contribution statement

F. Naqvi: Data curation, Formal analysis, Investigation, Methodology, Software, Validation, Visualization, Writing – original draft. **S. Karampagia:** Investigation, Methodology, Writing – original draft. **A. Spyrou:** Conceptualization, Funding acquisition, Investigation, Methodology, Project administration, Resources, Supervision, Writing – review & editing. **S.N. Liddick:** Conceptualization, Funding acquisition, Investigation, Methodology, Resources, Supervision, Writing – review & editing. **A.C. Dombos:** Investigation, Methodology, Resources, Software, Writing – original draft. **D.L. Bleuel:** Investigation, Writing – review & editing. **B.A. Brown:** Investigation, Supervision, Writing – review & editing. **L. Crespo Campo:** Investigation, Writing – review & editing. **A. Couture:** Investigation, Writing – review & editing. **B. Crider:** Investigation, Writing – review & editing. **T. Ginter:** Investigation, Resources, Writing – review & editing. **M. Guttormsen:** Conceptualization, Funding acquisition, Investigation, Methodology, Supervision, Writing – review & editing. **A.C. Larsen:** Conceptualization, Funding acquisition, Investigation, Methodology, Supervision, Writing – review & editing. **R. Lewis:** Investigation, Writing – review & editing. **P. Möller:** Investigation, Writing – review & editing. **S. Mosby:** Investigation, Writing – review & editing. **G. Perdikakis:** Investigation, Writing – review & editing. **C. Prokop:** Investigation, Writing – review & editing. **T. Renstrøm:** Investigation, Writing – review & editing. **S. Siem:** Investigation, Writing – review & editing.

Declaration of competing interest

The authors declare that they have no known competing financial interests or personal relationships that could have appeared to influence the work reported in this paper.

Acknowledgement

Authors sincerely thank the support of the NSCL accelerator staff. This work was supported by the National Science Foundation under Grants No. PHY 1350234 (CAREER), No. PHY 1102511 (NSCL), No. PHY 1811855, and No. PHY 0822648 (Joint Institute for Nuclear Astrophysics). We would also like to acknowledge the support of Department of Energy National Nuclear Security Administration (NNSA) under Grant No. DE-NA0002132 and Award No. DE-NA0003221 and the Nuclear Science and Security Consortium under Award No's. DE-NA0000979 and DE-NA0003180. A.C.L is thankful for the financial support through the ERC-STG-2014 under Grant Agreement No. 637686. The funding from the Research Council of Norway, Project Grant No. 205528 (A.C.L. and M.G.) and Project Grant No. 210007 (L.C.C, T.R, and S.S) is highly acknowledged. D.L.B. acknowledges the support of LLNL under Contract No. DE-AC52-07NA27344. The LANL work was supported by the NNSA of the U.S. Department of energy at Los Alamos National Laboratory under Contract No. DE-AC52-06NA25396.

References

[1] M. Bernas, Ph. Dessagne, M. Langevin, J. Payet, F. Pougheon, P. Roussel, Phys. Lett. B 113 (1982) 4.
[2] O. Perru, et al., Phys. Rev. Lett. 96 (2006) 232501.
[3] B.P. Crider, et al., Phys. Lett. B 763 (2016) 108.
[4] M. Vergnes, et al., Phys. Lett. B 72 (1978) 447.
[5] G. Rotbard, et al., Nucl. Phys. A 401 (1983) 41.
[6] R. Lecomte, M. Irshad, S. Landsberger, G. Kajrys, P. Paradis, S. Monaro, Phys. Rev. C 22 (1980) 2420.
[7] E. Nolte, et al., Z. Phys. 268 (1974) 267.
[8] S. Franchoo, et al., Phys. Rev. Lett. 81 (1998) 3100.
[9] H. Grawe, in: The Euroschool Lectures on Physics with Exotic Bemas, vol. 1, in: Lecture Notes in Physics, vol. 651, Springer, Berlin-Heidelberg, 2004, p. 33.
[10] N.A. Smirnova, A. DeMaesschalck, A. VanDyck, L. Heyde, Phys. Rev. C 69 (2004) 044306.
[11] T. Otsuka, T. Suzuki, R. Fujimoto, H. Grawe, Y. Akaishi, Phys. Rev. Lett. 95 (2005) 232502.
[12] F. Nowacki, A. Poves, E. Caurier, B. Bounthong, Phys. Rev. Lett. 117 (2016) 272501.
[13] M. Huhta, P.F. Mantica, D.W. Anthony, P.A. Lofy, J.I. Prisciandaro, R.M. Ronningen, M. Steiner, W.B. Walters, Phys. Rev. C 58 (1998) 3187.
[14] S.V. Ilyushkin, et al., Phys. Rev. C 80 (2009) 054304.
[15] S.V. Ilyushkin, et al., Phys. Rev. C 83 (2011) 014322.
[16] N. Patronis, et al., Phys. Rev. C 80 (2009) 034307.
[17] S. Franchoo, et al., Phys. Rev. C 64 (2001) 054308.
[18] K.T. Flanagan, et al., Phys. Rev. Lett. 103 (2009) 142501.
[19] J.L. Tracy Jr., et al., Phys. Rev. C 98 (2018) 034309.
[20] J.V. Roosbroeck, et al., Phys. Rev. C 71 (2005) 054307.
[21] J.C. Hardy, L.C. Carraz, B. Jonson, P.G. Hanse, Phys. Lett. B 71 (1977) 307.
[22] B. Rubio, W. Gellettly, E. Nácher, A. Algora, J.L. Tain, A. Pérez, L. Caballero, J. Phys. G 31 (2005) S1477.
[23] Y. Fujita, B. Rubio, W. Gelletly, Prog. Part. Nucl. Phys. 66 (2011) 549.
[24] E.M. Burbridge, G.R. Burbridge, W.A. Fowler, F. Hoyle, Rev. Mod. Phys. 29 (1957) 547.
[25] P. Hosmer, et al., Phys. Rev. C 82 (2010) 025806.
[26] M. Mumpower, R. Surman, G.C. McLaughling, A. Aprahamian, Prog. Part. Nucl. Phys. 86 (2016) 86.
[27] R. Surman, M. Mumpower, R. Sinclair, K.L. Jones, W.R. Hix, G.C. McLaughling, AIP Adv. 4 (2014) 041008.
[28] J.J. Cowan, F.-K. Thielemann, J.W. Truran, Phys. Rep. 208 (1991) 267.

[29] A. Algora, J.L. Tain, B. Rubio, M. Fallot, W. Gelletly, Eur. Phys. J. A 85 (2021) 57.
[30] S.R. Stroberg, et al., Phys. Rev. C 90 (2014) 034301.
[31] J.L. Tain, et al., Phys. Rev. Lett. 115 (2015) 062502.
[32] R. Dungan, et al., Phys. Rev. C 93 (2016) 021302(R).
[33] A. Spyrou, et al., Phys. Rev. Lett. 117 (2016) 142701.
[34] V. Vaquero, et al., Phys. Rev. Lett. 118 (2017) 202502.
[35] M. Honma, T. Otsuka, T. Mizusaki, M. Hjorth-Jensen, Phys. Rev. C 80 (2009) 064323.
[36] E. Manè, et al., Phys. Rev. C 84 (2011) 024303.
[37] P. Möller, J. Nix, K.-L. Kratz, At. Data Nucl. Data Tables 66 (1997) 131.
[38] D.J. Morrissey, B.M. Sherrill, M. Steiner, A. Stolz, I. Wiedenhoever, Nucl. Instrum. Methods Phys. Res., Sect. B 204 (2003) 90.
[39] A. Simon, et al., Nucl. Instrum. Methods Phys. Res., Sect. A 703 (2013) 16.
[40] S.N. Liddick, et al., Phys. Rev. Lett. 116 (2016) 242502.
[41] B. Singh, A.R. Farhan, Nucl. Data Sheets 107 (2006) 1923.
[42] A. Negret, B. Singh, Nucl. Data Sheets 114 (2013) 841.
[43] E. Lund, B. Erkström, B. Fogelberg, G. Rudstam, in: Contrib. Proc. 5^{th} Int. Conf. Nuclei Far from Stability, Rosseau Lake, Canada, E6, 1987.
[44] J.A. Winger, John C. Hill, F.K. Wohn, E.K. Warburton, R.L. Gill, A. Piotrowski, D.S. Brenner, Phys. Rev. C 39 (1989) 1976.
[45] M. Bernas, P. Armbruster, J.P. Bocquet, R. Brissot, H. Faust, Ch. Kozhuharov, J.L. Sida, Z. Phys. A 336 (1990) 41.
[46] K.-L. Kratz, et al., Z. Phys. A 340 (1991) 419.
[47] P.L. Reeder, R.A. Warner, R.M. Liebsch, R.L. Gill, A. Piotrowski, Phys. Rev. C 31 (1985) 1029.
[48] S. Agostinelli, J. Allison, K. Amako, et al., Nucl. Instrum. Methods Phys. Res., Sect. A 506 (2003) 250.
[49] A.C. Dombos, et al., Phys. Rev. C 93 (2016) 064317.
[50] F. Bečvář, Nucl. Instrum. Methods Phys. Res., Sect. A 417 (1998) 434.
[51] B. Pfeiffer, K.-L. Kratz, P. Möller, Prog. Nucl. Energy 41 (1–4) (2002) 39.
[52] I.N. Borzov, Phys. Rev. C 71 (2005) 065801.
[53] B.A. Brown, W.D.M. Rae, Nucl. Data Sheets 120 (2014) 115.
[54] B.H. Wildenthal, M.S. Curtin, B.A. Brown, Phys. Rev. C 28 (1983) 1343.
[55] K.L. Haglin, Phys. Rev. C 53 (1996) R2606(R).